

Noninvariance of Space- and Time-Scale Ranges under a Lorentz Transformation and the Implications for the Study of Relativistic Interactions

J.-L. Vay*

Lawrence Berkeley National Laboratory, Berkeley, California 94720, USA

(Received 16 January 2007; published 30 March 2007)

We present an analysis which shows that the ranges of space and time scales spanned by a system are not invariant under Lorentz transformation. This implies the existence of a frame of reference which minimizes an aggregate measure of the range of space and time scales. Such a frame is derived, for example, for the following cases: free electron laser, laser-plasma accelerator, and particle beams interacting with electron clouds. The implications for experimental, theoretical, and numerical studies are discussed. The most immediate relevance is the reduction by orders of magnitude in computer simulation run times for such systems.

DOI: [10.1103/PhysRevLett.98.130405](https://doi.org/10.1103/PhysRevLett.98.130405)

PACS numbers: 03.30.+p, 02.70.-c, 52.40.Mj

The study of the interaction of two or more “objects” (in the broad sense of collections of particles, possibly including massless particles such as photons, or wave packets) crossing each other at relativistic velocities is common to many areas of science and technology. This field encompasses all laser-matter interactions and relativistic beams colliding with each other or interacting with matter. In many instances, the system exhibits a disparity of space and time scales between the crossing objects which can span several orders of magnitude, with implications for experimentation, theoretical, and numerical analysis. Examples of such systems with large separations of scales are free electron lasers [1], laser-plasma acceleration [2–4], and high-energy particle beams interacting with electron clouds [5].

The disparity of scales sets significant constraints on experiments where a very short particle and/or laser beam propagates through a structure (plasma, accelerator, ...) which is orders of magnitude longer. The increase in energy of the incident pulse, coupled to a decrease in the pulse duration, puts increasingly challenging requirements on the precision of apparatus alignment, time response, and synchronism.

For the theoretical study of such systems, it is common practice to perform a change of variable of the form $\{x' = x - vt, t' = t\}$ or $\{x' = x, t' = t - x/v\}$, where t is the time, x is the direction of propagation of the incident beam, and v is its speed in the laboratory frame. This allows the study of just a “window” moving, respectively, in space (time) which encompasses the “beam” and that portion of the “target” which it is instantaneously overlapping. It is also recognized that the separation of scales in space and time between the incident beam and the target offers the opportunity for simplifying the mathematical description of the interaction through the use of Eikonal (sometimes referred to as “slowly varying envelope”) approximations. Although the simplification allows recovery of many features of the physical processes at play, there are instances where the physics that is omitted by these

models cannot be neglected, and numerical solutions on a computer are then required. Because a wide separation of space and time scales can impose severe limitations on the size of the system that can be modeled (“multiscale” problems), these usually require massively parallel computations, and parametric studies of the full system are often impossible without the use of the above-mentioned approximations.

We will show that the use of the Lorentz transformation $\{x' = \gamma(x - vt), t' = \gamma(t - vx/c^2)\}$ (where c is the speed of light in vacuum and $\gamma = 1/\sqrt{1 - v^2/c^2}$ is the usual relativistic factor) offers the opportunity of bridging disparate space and time scales, the benefits of which will be discussed and demonstrated on one example.

We begin by illustrating the effect of scale separation under the Lorentz transformation on a very simple configuration where we consider two objects with parallel velocity vectors having, in a frame of reference F_0 : the same (a) length l , (b) minimum length of interest λ , and (c) maximum frequency of interest $\nu = 1/\tau$; and different speed $\beta_+ \geq 0$ and $\beta_- \leq 0$ (denoting quantities related to the two objects, respectively, with the subscripts + and -). For the sake of simplicity, and for this example only, we assume that the two objects are sufficiently rigid macroscopically that the total length and average velocities are not affected during the interaction. Under these assumptions, the total time for the two objects to cross each other in the frame F_0 is given by $T = 2l/(|\beta_+ - \beta_-|c)$, and the ratios of the longest to smallest space/time scales are given, respectively, by $R_s = 2l/\lambda$ and $R_t = T/\tau$. In a frame F moving at speed βc in F_0 , we have (denoting quantities in the moving frame with the superscript *)

$$\begin{aligned} \beta_{\pm}^* &= (\beta_{\pm} - \beta)/(1 - \beta\beta_{\pm}), \\ l_{\pm}^*/l &= \lambda_{\pm}^*/\lambda = \tau/\tau_{\pm}^* = 1/[\gamma(1 - \beta\beta_{\pm})], \\ T^* &= (l_+^* + l_-^*)/[|\beta_+^* - \beta_-^*|c], \end{aligned} \quad (1)$$

where $\gamma = 1/\sqrt{1 - \beta^2}$.

If we assume that $\beta \geq 0$ then we have $\lambda_-^* \leq \lambda_+^*$ and $\tau_+^* \leq \tau_-^*$, so that the ratios of longest to smallest space and time scales are given in the moving frame F by

$$R_s^* = (l_+^* + l_-^*)/\lambda_-^*, \quad R_t^* = T^*/\tau_+^*. \quad (2)$$

From (1) and (2), we find that the dependence Γ of space and time scales ratios with regard to the moving frame is given by

$$\Gamma = R_s^*/R_s = R_t^*/R_t = \frac{1 - \beta\bar{\beta}}{1 - \beta\beta_+}, \quad (3)$$

with $\bar{\beta} = (\beta_+ + \beta_-)/2$. If we assume $\bar{\beta} \ll 1$ (velocities of the two objects are almost equal and opposite in F_0), Γ simplifies to $\Gamma \approx 1/(1 - \beta\beta_+)$, which is plotted versus γ on Fig. 1 for several values of $\gamma_+ = 1/\sqrt{1 - \beta_+^2}$. It varies as $2\gamma^2$ for $\gamma < \gamma_+$ and asymptotes to $2\gamma_+^2$ for $\gamma > \gamma_+$.

From this, we conclude that the space and time scales associated with each beam, which span the same range in F_0 , separate from each other in a frame F moving at some velocity βc from F_0 , at the rate $\gamma^2 = 1/(1 - \beta^2)$. Note that this is general and applies to both particles and photons (for example, if object 1 is made of photons, we have $\beta_+ = \beta_-^* = 1$).

Figure 2 shows the space-time diagrams of two objects crossing each other (for this example, the velocities were such that the relativistic factor $\gamma_0 = 2$ for each object in F_0 ; but this choice is unimportant to the argument). The two objects that are represented can be viewed as entire uniform beams crossing each other or, perhaps more interestingly, as the smallest space-time unit of interest for each. Assuming that the two objects are identical in F_0 , the corresponding space-time diagram, shown in Fig. 2(a), is very simple, with geometrical structures at one scale only. In the rest frame F of one of the beams, the space-time diagram, shown in Fig. 2(b), reveals a more “complex” layout with very disparate space and time scales, revealing graphically the separation of scales obtained above via mathematical analysis. We also remark that the space-time area covering the interaction (usually of most interest), is given by the overlap of the two objects (shaded

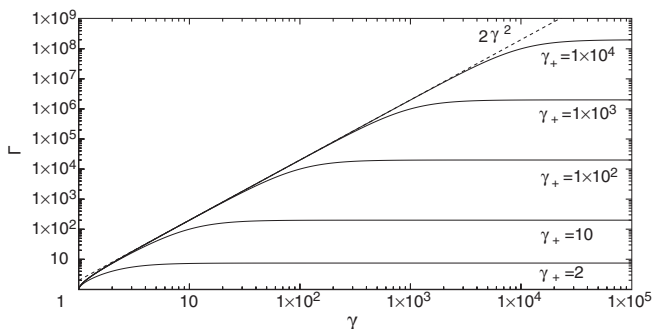


FIG. 1. Γ as a function of γ for $\gamma_+ = \{2, 10, 1 \times 10^2, 1 \times 10^3, 1 \times 10^4\}$.

areas on Fig. 2), which occupies a maximal fraction of the support of the system in F_0 , when the disparity of scales is minimal. Finally, we note that the diagram in Fig. 2(b) can be representative of a short particle beam or laser pulse propagating into a long structure, such as a free-electron laser, a laser-plasma accelerator, or of a beam interacting with an electron cloud in a particle accelerator, which are considered below.

These considerations have consequences in the experimental, theoretical, and numerical study of a system. Experimentally, the study of the fundamental mechanisms of the interactions might be greatly simplified if performed in the frame which minimizes the range of scales. Potential advantages are (a) the system is more compact spatially, (b) the time of interaction is shorter, (c) the ratios between largest to smallest space and time scales are minimized. All of these alleviate the requirements on alignment, time response of diagnostics, and synchronism. Theoretically, it is common practice to study particle beams in their “rest” or “bucket” frames where the analysis can be greatly simplified [6]. Furthermore, developments in series (for example) around some spatial, time, frequency, or wavelength of interest might offer different opportunities of approximation, depending on the chosen frame of analysis, which have different tradeoffs with regards to the study of some aspects of the mechanisms at play.

The most important immediate application probably lies in the numerical modeling of such systems. The approximations used theoretically (Eikonal, “slowly varying envelope,” “quasistatic”) are also used in numerical analysis in order to reduce the requirements on the number of points in space and time of the discretized system (using Eulerian or Lagrangian methods). However, these approximations are sometimes inappropriate and the system must be modeled from first principles, but the range of the space and time scales imposes very severe limitations. In such cases, it may be very advantageous to perform the calculation in

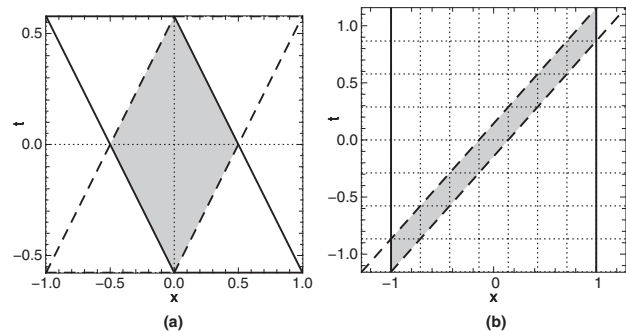


FIG. 2. Phase-space diagrams of two identical rigid objects crossing each other as viewed in (a) the frame of the center of mass, (b) the rest frame of one object (solid line—object 1, dashed line—object 2, shaded area—overlap of bodies). A regular mesh (dotted lines), with cells resolving the smallest space and time scales, is overlaid.

the frame which minimizes the range of scales. Potential complications include the modeling of internal boundaries moving at relativistic velocities or the existence of a non-inertial moving frame (in a case of a beam propagating in a circular accelerator, for example). However, the dependence of Γ on the square of γ indicates that gains of orders of magnitude are possible for relative velocities with large γ , offsetting the potential difficulties.

As a first example, let us consider one pass of a free electron laser configuration [1] where an electron beam of length l propagates at speed v into a wiggler consisting of N magnet pairs of periodicity length λ_w and vector potential A_w , with $l \ll \lambda_w$. When crossing the wiggler, the electron beam will emit electromagnetic radiation at the wavelength $\lambda = \lambda_w[(1 + a_w^2)/(2\gamma^2)]$, where $a_w = eA_w/(mc^2)$, and e and m are, respectively, the charge and mass of the electron. The time T taken by the driver beam to propagate through the magnets is given by $T \approx N\lambda_w/v$. Finally, the ratios of the longest to smallest space/time scales are given, respectively, by $R_s = N\lambda_w/\lambda \propto \gamma^2$ and $R_t = T/(\lambda/c) = N\lambda_w c/(\lambda v) \propto \gamma^2$. Hence both ratios of scales vary as the square of the relativistic factor γ which, for large values of γ , corresponds to a large separation of space and time scales. If we consider now the same system in a frame moving at speed v relative to the laboratory frame, and applying the Lorentz transformation, the quantities become, in this frame, $\lambda^*/\lambda = \lambda_w/\lambda_w^* = \gamma$ and $R_s^* = R_s/\gamma^2 \propto 1$. Hence in this frame of reference, the disparity of space and time scales vanishes [7].

As a second example, let us now consider a laser-plasma wakefield accelerator (LPWA) scheme [2–4] where an incident laser pulse of wavelength λ and length l propagates through a neutral plasma of length L_p and density n_0 . The highest frequency of interest is $\omega = 2\pi c/\lambda$, while the time of the interaction is given by $T = (L_p + l)/c$. The ratios of space (time) scales are, respectively, $R_s = (L_p + l)/\lambda$ and $R_t = T/(2\pi/\omega) = R_s$. In a frame moving at relativistic speed $v = \beta c$ relative to the laboratory frame, we have the following (note that we make the common assumption that the backward Raman emission can be neglected; if not, further considerations are needed that will be addressed elsewhere): $L_p/L_p^* = \gamma$, $\lambda^*/\lambda = l^*/l = \omega/\omega^* = \gamma(1 + \beta)$, so that $T^* = (l^* + L_p^*)/(c + v)$, $R_s^* = (L_p^* + l^*)/\lambda^* = \alpha R_s$, and $R_t^* = T^*/(2\pi/\omega^*) = \alpha R_t/(1 + \beta)$, with $\alpha = (1 - \beta + l/L_p)/(1 + l/L_p)$. We have $\alpha = 1$ when $\beta = 0$, $\alpha \propto 1/\gamma^2$ when $\gamma^2 \ll L_p/l$, and $\alpha \approx \frac{3}{2}l/L_p$ when $\gamma^2 = L_p/l$. Since typically, $L_p \gg l$, the ratio of length and space scales can be considerably reduced in the moving frame [8].

As a last example, let us consider a relativistic particle beam of length l , positively charged, propagating at speed $\beta_b c$ in a linear periodic section of an accelerator structure of length L and periodicity $\lambda = L/n$, and interacting with electrons emitted by photoemission and/or secondary emission at the walls of the vacuum pipe [5]. For very

short bunches $l \ll L$, the minimum (maximum) space scales are given by the bunch (accelerator) section lengths l and L . The minimum time scale in the laboratory frame is given by the transit time τ of an electron across the pipe due to the beam electric field. The maximum time scale T is given by the time taken by the beam to get across the accelerator section and we have $T = (L + l)/(\beta_b c)$ where we have assumed that there are no large accelerating fields in the section. We have then $R_s = (L + l)/l$ and $R_t = T/\tau$. In a frame moving at relativistic speed βc relative to the laboratory frame, the quantities become $l^* = l/[\gamma(1 - \beta\beta_b)]$, $L/L^* = \tau^*/\tau = \gamma$, and $T^* = (L^* + l^*)/[(\beta + \beta_b)c]$, so that

$$R_s^* = \frac{L^* + l^*}{l^*} = R_s \frac{1 + l/L - \beta\beta_b}{1 + l/L},$$

$$R_t^* = T^*/\tau^* = R_t \frac{\beta_b(1 + l/L - \beta\beta_b)}{\gamma^2(1 + l/L)(\beta + \beta_b)(1 - \beta\beta_b)}. \quad (4)$$

For ultrarelativistic beams ($\beta_b \rightarrow 1$), then $R_s^*/R_s \rightarrow R_t^*/R_t \rightarrow (1 - \beta + l/L)/(1 + l/L)$ which is the same function α obtained for the LPWA case. The conclusion obtained for the LPWA case thus holds here.

We illustrate (using the WARP code [10]) the dramatic speedup which can be obtained, in a numerical simulation of a beam of 10^{12} protons propagating at $\gamma = 500$ (in the

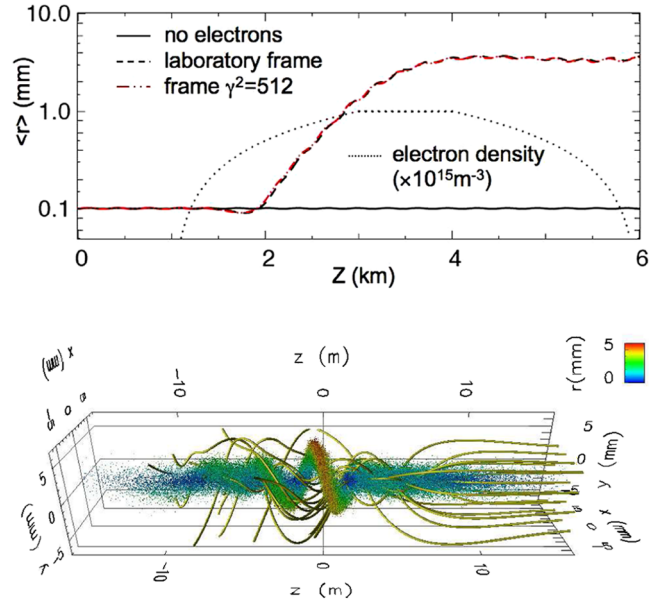


FIG. 3 (color online). (Top) average value of the beam radius for a thin slice taken in the middle of the beam, as a function of its position in the laboratory frame, given for three runs: (a) no electrons, (b) with electrons, in the laboratory frame, and (c) with electrons, in a frame moving at $\gamma = \sqrt{512}$. (Bottom) 3D snapshot of the beam and electrons from run in the moving frame taken when the head of the beam reaches $z = 4$ km in the laboratory frame [beam macroparticles are rendered as spheres colored according to their position in $r(\text{mm})$; electrons are sampled and rendered as streamlines in gold color (or gray)].

laboratory) into a cylindrical pipe of radius $R = 1$ cm, embedded into an external continuous focusing azimuthal magnetic field $B_\theta = 0.15r$, where r is the distance to the axis of propagation. After 1 km of propagation through vacuum, the beam encounters an initially cold background of electrons with uniform density, which ramps linearly over 2 km from zero to a maximum of $n_e = 10^{15} \text{ m}^{-3}$, and then remains constant for 1 km before dropping back to zero linearly over 2 km. The beam distribution is initially 6D Gaussian with an rms transverse size $\sigma_x = \sigma_y = 1$ mm, rms length $\sigma_z = 10$ cm, beta functions $\beta_x = \beta_y = 100$ m, and no momentum spread. The beam is injected such that each slice passing through $z = 0$ has the above-mentioned characteristics, initial offset $x_{\text{off}} = 0.1\sigma_x$ and velocity $v_y = 0.1v_{\text{th}}$, where v_{th} is the initial transverse thermal spread. The average value of the beam radius $\langle r \rangle = \langle \sqrt{x^2 + y^2} \rangle$, for a thin slice taken in the middle of the beam, as a function of its position in the laboratory frame, is given in Fig. 3 (top) for three runs: (a) with no electrons, (b) with electrons, in the laboratory frame, and (c) with electrons, in a frame moving at $\gamma = \sqrt{512}$. As the beam propagates through the background of electrons, the interaction leads to a type of hose instability (see bottom of Fig. 3) which is characterized by an exponential growth of $\langle r \rangle$, followed by saturation. As expected, the two calculations performed with electrons led to the same results. However, due to the different ratios of space and time scales, the Courant condition on the motion of electrons led to very different restrictions on the time steps: in the laboratory frame, the calculation required over 5×10^6 time steps and over a week of clock time, running on eight 2.2 GHz Opteron processors; while the calculation in the frame moving at $\gamma = \sqrt{512}$ required only approximately 5000 time steps and completed in less than 30 min, using the same computer resources.

In conclusion, we have shown that, for a system which contains a component of matter and/or light moving at relativistic velocities with regard to another component, there is a preferred frame of reference which minimizes the ranges of space and time scales, and the ratio of maximum to minimum space or time scales varies as the square of the relativistic factor γ associated with the speed of the moving frame. We have also shown that the large space and time-scale separations in several systems of experimental interest vanish in this preferred frame, and discussed new possibilities offered by this effect for the experimental, theoretical, and numerical study of these configurations. We have demonstrated the effect on three examples: free electron laser, laser-plasma acceleration, and electron

cloud interactions with high-energy beams. Furthermore, we have recovered for each of these examples the dependence on the square of the relativistic factor γ which was obtained for a simpler symmetric configuration. We note, in particular, that the modeling of these systems using computer simulations can benefit from orders of magnitude reduction in run time when performed in this preferred frame, and offered an example where a speedup of 3 orders of magnitude was obtained.

The author acknowledges fruitful discussions with J. J. Barnard, D. L. Bruhwiler, J. R. Cary, C. M. Celata, R. H. Cohen, P. Colella, R. C. Davidson, E. H. Esarey, W. M. Fawley, A. Friedman, M. A. Furman, E. P. Lee, W. P. Leemans, B. G. Logan, S. M. Lund, A. W. Molvik, W. B. Mori, R. D. Ryne, P. A. Seidl, A. M. Sessler, B. A. Shadwick, K. G. Sonnad, M. Venturini, and J. S. Wurtele. This work was supported by the Director, Office of Science, Office of Fusion Energy Sciences, of the U.S. Department of Energy under Contract No. DE-AC02-05CH11231 and by the U.S.-LHC Accelerator Research Program (LARP).

*Electronic address: jlvay@lbl.gov

- [1] N. M. Kroll, P. L. Morton, and M. N. Rosenbluth, *IEEE J. Quantum Electron.* **17**, 1436 (1981).
- [2] C. G. R. Geddes *et al.*, *Nature (London)* **431**, 538 (2004).
- [3] S. P. D. Mangles *et al.*, *Nature (London)* **431**, 535 (2004).
- [4] J. Faure *et al.*, *Nature (London)* **431**, 541 (2004).
- [5] *Proceedings of the 31st ICFA Advanced Beam Dynamics Workshop on Electron-Cloud Effects (ECLLOUD'04), Napa, California, 2004* (CERN Report No. CERN-2005-001, 2005); <http://icfa-ecloud04.web.cern.ch/icfa-ecloud04/agenda.html>
- [6] R. C. Davidson, *Phys. Rev. Lett.* **81**, 991 (1998).
- [7] Because of the use of the Lorentz transformation, the frame used here is not equivalent to the so-called bucket frame.
- [8] During the final writing of this Letter, it was brought to the attention of the author [9] that the calculation of the LWFA and PBWA schemes in a Lorentz boosted frame was considered earlier (~ 1994) and tried in one-dimension using the code WAVE. While it did show some promise, issues related to large amplitude short wavelength fields arose that were tentatively attributed to reflected light or unresolved Raman backscatter. As a consequence, the project was discontinued.
- [9] W. B. Mori and T. Katsouleas (private communication).
- [10] D. P. Grote, A. Friedman, J.-L. Vay, and I. Haber, *AIP Conf. Proc.* **749**, 55 (2005).